Evaluation of Instability of a Low-salinity Density-dependent Flow in a Porous Medium

Y. T. Habtemichael*[1], R. T. Kiflemariam[2], H. R. Fuentes[1]

[1]Civil and Environmental Engineering, Florida International University, Miami, FL, USA
[2]Mechanical and Materials Engineering, Florida International University, Miami, FL, USA
*Corresponding author: yhabt001@fiu.edu

Abstract: Seawater intrusion into coastal aquifers is usually modeled by using transport models that account for the effect of variable-density on flow. Variable-density models can be validated with the Henry and Elder benchmark problems. However, when mixed convective flow is simulated under variable density conditions, it is susceptible to physical and numerical instabilities. The purpose of this work is to explore the development of instability during the migration of a NaCl plume in a homogenous medium that is initially saturated with freshwater. This is done by varying the Peclet (Pe) and Rayleigh (Ra) numbers to represent different discretization and density contrasts, while selecting a Courant number (Cr) that gives numerical stability. COMSOL Multiphysics® is used to model concentration distribution of the NaCl plume and sensitivity of the output to different values of Pe and Ra numbers is evaluated.

Keywords: groundwater flow and transport, saltwater intrusion, instability, multiphysics, COMSOL

1. Introduction

Groundwater quality is threatened by leaching of contaminants from uncontrolled landfills and by saltwater intrusion in coastal aquifers. The contaminant transport and spreading is greatly influenced by density variations between the contaminant plume and the ambient water. Fluid density can vary with contaminant concentrations producing buoyancy flow. When a more dense fluid is enclosed by and moving along in a body of less dense fluid, fingering instabilities develop and play important role in the mixing and dispersion processes (Schincariol et al., 1994). Numerical errors in transport codes can also lead to development of instabilities which are physically unrealistic.

Variable-density models are commonly validated with the Henry and Elder benchmark problems. However, when mixed convective flow is simulated under variable density conditions, it is susceptible to physical and numerical instabilities. The model setup of Schincariol et al (1994) has been slightly modified and used as a bench mark to analyze physical instability in coupled flow and transport problems using MITSU3D and SUTRA (Ibaraki, 1998), and PHWAT (Mao et al., 2006). The following paper uses the same model set up as in Ibaraki (1998) and Mao et al. (2006) to investigate the occurrence of instability using COMSOL MultiPhysics®.

2. Model Description

The benchmark involves migration of a plume (NaCl) through a porous medium initially saturated with freshwater. The model domain is a rectangular region 1m in width and 0.5m in depth. The physical system of the model domain is shown in figure 1 and the physical parameters are given in Ibaraki (1998) and shown in table 1.

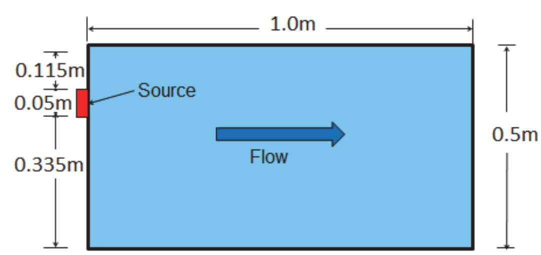

Figure 1. Configuration of the model domain (Ibaraki, 1998)

Table 1: Parameter values for numerical simulations (Ibaraki, 1998)

Parameter	Value
Permeability	5.7×10^{-11} m^2
Porosity	0.38
Free-solution diffusion coefficient	1.61×10^{-9} m^2 s^{-1}
Groundwater velocity	2.75×10^{-6} m s^{-1}
Longitudinal dispersivity	3.0×10^{-4} m
Transverse dispersivity	0.0 m
Tortuosity	0.35
Viscosity	
Water	1.002×10^{-3} pa s
1000 mg/l NaCl solution	1.004×10^{-3} pa s
2000 mg/l NaCl solution	1.006×10^{-3} pa s
3000 mg/l NaCl solution	1.008×10^{-3} pa s
5000 mg/l NaCl solution	1.011×10^{-3} pa s
Relative density	
Water	0.9982 g cm^{-3}
1000 mg/l NaCl solution	0.9989 g cm^{-3}
2000 mg/l NaCl solution	0.9997 g cm^{-3}
3000 mg/l NaCl solution	1.0004 g cm^{-3}
5000 mg/l NaCl solution	1.0018 g cm^{-3}

3. Governing Equations

Fluid flow and solute transport equations are needed to describe solute-driven density dependent flow. The flow is described using Darcy's law:

$$\frac{\partial \varepsilon \rho}{\partial t} + \nabla \cdot \rho \mathbf{u} = 0$$

where ε and ρ [ML^{-3}] are the porosity and density of the fluid, respectively, and t is the time [T]. The fluid velocity ($\mathbf{u}$ [LT^{-1}]) is given by:

$$\mathbf{u} = \frac{\kappa}{\mu}(\nabla p + \rho g \nabla D)$$

where κ [L^2] is the permeability of the rock matrix, μ [ML^{-1}T^{-1}] is the viscosity of the fluid, p [ML^{-1}T^{-2}] is the pressure and g[LT^{-2}] is the gravitational acceleration. The gradient of D [L] indicates the direction of the vertical coordinate, y.

The governing equation for solute transport is the advection-dispersion equation written as:

$$\frac{\partial \theta_s c}{\partial t} + \nabla \cdot (c\mathbf{u}) - \nabla \cdot (\theta_s \tau D_{ij} \nabla c) = 0$$

where c[ML^{-3}] is the concentration of solute, θ_s is the fluid's volume fraction ($\theta_s = \varepsilon$, for saturated flow), and D_{ij} [L^{2}T^{-1}] is the fluid's diffusion coefficient expressed as (Ibaraki, 1998):

$$\theta_s D_{ij} = (\alpha_l - \alpha_t)\frac{u_i u_j}{|u|} + \alpha_t |u| \delta_{ij} + \theta_s \tau D_d \delta_{ij}$$

α_l [L] and α_t [L] are the longitudinal and transverse dispersivities, respectively, δ_{ij} is the Kronecker delta, τ is the matrix tortuosity and D_d [L^{2}T^{-1}] is the free-solution diffusion coefficient.

4. Use of COMSOL Multiphysics

COMSOL is used to solve the coupled flow and transport equations. Thus the study uses the Darcy (*dl*) and solute transport (*esst*) modes of COMSOL. The two equations are coupled by density and velocity. Also, fluid density and viscosity are greatly affected by solute concentration and are expressed as functions of concentration (Boufadel et al., 1999), giving similar values as in table 1. Taking the reference density (ρ_0) and viscosity (μ_0) of freshwater, the equations of state are:

$$\rho = \rho_0 (1 + 6.46 \times 10^{-7} c)$$

$$\mu = \frac{\mu_0}{(1 - 1.566 \times 10^{-6} c)}$$

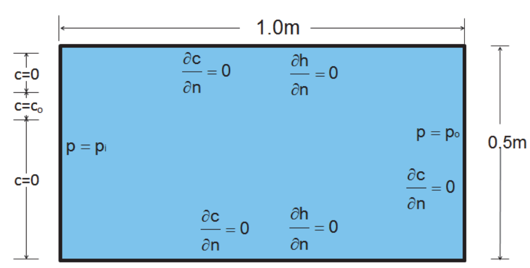

Figure 2. Model boundary conditions

The model domain is bound by no-flow boundaries on the top and bottom. Constant pressure values are assigned to the left and right boundaries to provide an average linear groundwater velocity of 2.75×10^{-6} m/s. For solute transport, the nodes at the source are assigned the given concentration. The nodes on the left side boundary, away from the source, are assigned a value of 0 mg/L. All the remaining boundaries are assumed no-flux boundaries.

Simulations are carried for different spatial and temporal discretization by varying the Pe and Cr numbers, respectively, given by:

$$\mathrm{P}e = \frac{\mathrm{v}\Delta l}{D}$$

$$\mathrm{Cr} = \frac{\mathrm{v}\Delta t}{\Delta l}$$

where v $[LT^{-1}]$ is the fluid velocity, D $[L^2T^{-1}]$ is dispersion coefficient, and Δl [L] and Δt [T] are the grid size and time step, respectively.

A structured meshing is used with coarse grids (100 by 50 elements) and fine grids (200 by 100 elements). This meshing corresponds to Pe of 11 and 5.5, respectively. Fixed time steps are used by specifying the same initial and final time steps in COMSOL. The analysis is done for time steps of 300 s and 1800 s. The grid sizes and time steps used are similar to those used in Mao et al. (2006) and the source concentrations evaluated are for 1000 mg/L and 2000 mg/L.

5. Results

Results did not converge for high density contrasts (e.g., source concentration of 10,000 mg/L) even for very fine mesh configurations and small time steps. In fact, simulation of instability from high density contrasts is still a numerically challenging problem (Mao et al., 2006). Thus the instability is evaluated under low density contrasts (i.e., for source concentrations of 1000 mg/L and 2000 mg/L). Figure 3 shows the concentration distribution with Pe of 11 and figure 4 shows the distribution for Pe of 5.5. In figure 3, the time steps of 1800 s and 300 s represent Cr numbers of 0.5 and 0.08, respectively. In figure 2, the corresponding Cr numbers are about 1 and 0.17. All the values of Cr are less or equal to 1 and satisfy the general numerical stability criteria. A single unstable 'lobe' develops at the front of the plume for a source concentration of 1000 mg/L. This lobe shows no visible difference with varying Cr and Pe numbers. When the source plume is increased to 2000 mg/L, more instability is developed with unstable lobes appearing on the front and in the middle of the plume. The physical instability is usually in the front of the plume and additional lobes in the middle of the plume indicate some numerical instability. The modified Rayleigh number for the 2000 mg/L concentration is in the unstable flow range (Mao et al., 2006) and the results obtained are as expected. The instability (number of lobes) decreases with decreasing Cr number and is reduced further with the finer mesh.

6. Conclusions

With a source concentration of 1000 mg/L, physical instability results in a single lobe at the front of the plume. Higher density contrast, with source concentration of 2000 mg/L, results in more than one lobe due to the additional effects of numerical instability. The number of lobes is reduced by using smaller grid sizes and time steps.

7. References

1. X. Mao, H. Prommer, D. Barry, C. D. Langevin, B. Panteleit and L. Li, "Three-dimensional model for multi-component reactive transport with variable density groundwater flow," *Environmental Modelling & Software,* **vol. 21**, pp. 615-628, (2006).

2. M. Ibaraki, "A robust and efficient numerical model for analyses of density-dependent flow in porous media," *J. Contam. Hydrol.,* **vol. 34**, pp. 235-246, (1998).

3. J. L. Musuuza, S. Attinger and F. A. Radu, "An extended stability criterion for density-driven flows in homogeneous porous media," *Adv. Water Resour.,* **vol. 32**, pp. 796-808, (2009).

4. R. A. Schincariol, F. W. Schwartz and C. A. Mendoza, "On the generation of instabilities in variable density flow," *Water Resour. Res.,* **vol. 30**, pp. 913-927, (1994).

5. M. C. Boufadel, M. T. Suidan and A. D. Venosa, "A numerical model for density-and-viscosity-dependent flows in two-dimensional variably saturated porous media," *J. Contam. Hydrol.,* **vol. 37**, pp. 1-20, (1999).

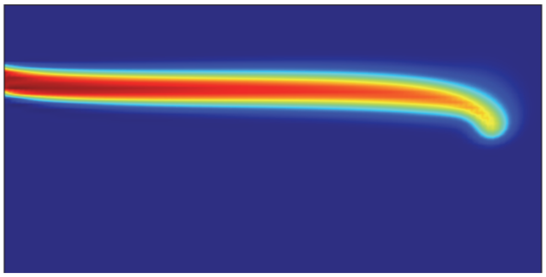

(a) C_{in} = 1000 mg/L, Δt = 1800 s (Cr=0.5)

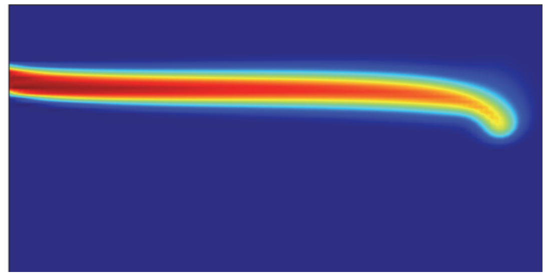

(b) C_{in} = 1000 mg/L, Δt = 300 s (Cr=0.08)

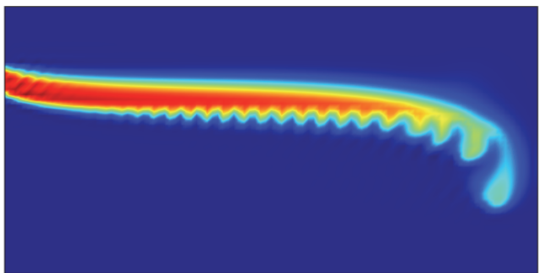

(c) C_{in} = 2000 mg/L, Δt = 1800 s (Cr=0.5)

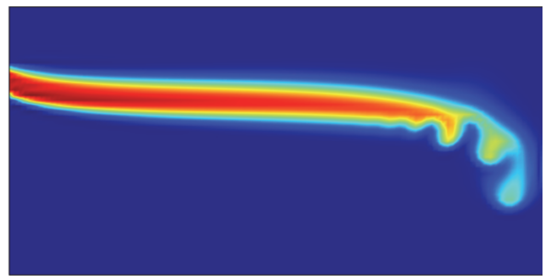

(d) C_{in} = 2000 mg/L, Δt = 300 s (Cr=0.08)

Figure 3. Plume concentration distributions after 90 h with grid size: 10 mm x 10 mm

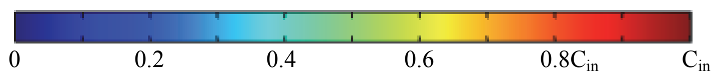

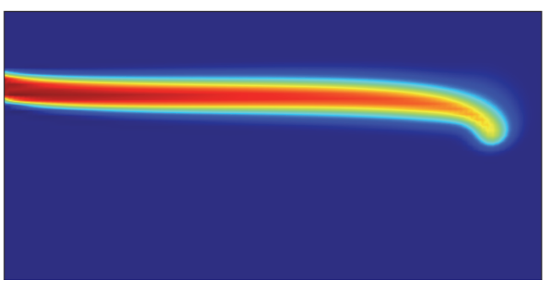

(a) C_{in} = 1000 mg/L, Δt = 1800 s (Cr=1)

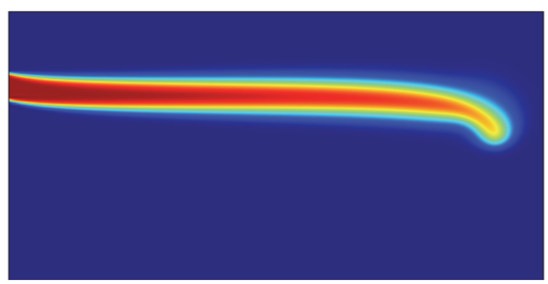

(b) C_{in} = 1000 mg/L, Δt = 300 s (Cr=0.17)

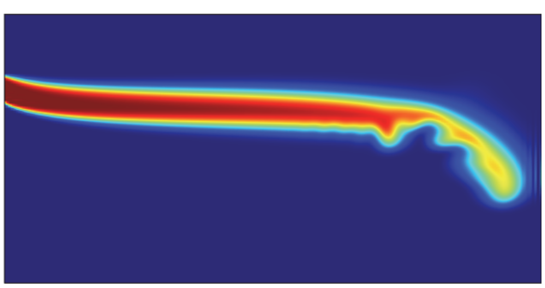

(c) C_{in} = 2000 mg/L, Δt = 1800 s (Cr=1)

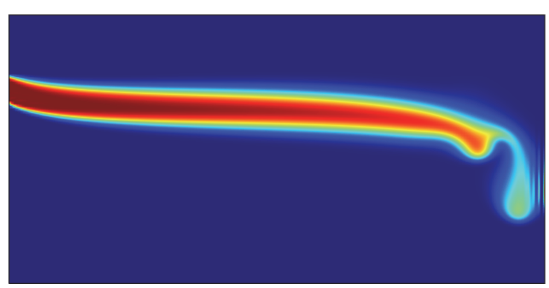

(d) C_{in} = 2000 mg/L, Δt = 300 s (Cr=0.17)

Figure 4. Plume concentration distributions after 90 h with grid size: 5 mm x 5 mm